BIFURCATION ANALYSES OF IN-PHASE AND OUT-OF-PHASE OSCILLATIONS IN BWRs

Quan Zhou and Rizwan-uddin
Department of Nuclear, Plasma, and Radiological Engineering
University of Illinois
103 South Goodwin Avenue
Urbana, Illinois 61801 U.S.A.
quanzhou@uiuc.edu, rizwan@uiuc.edu

ABSTRACT

Stability and bifurcation analysis of BWRs have been carried out using a reduced order two-channel model developed earlier by Karve et al. This model includes fuel rod heat conduction, single- and two-phase flow, and fundamental and first azimuthal mode modal neutron kinetics based on the ω-mode approach. The set of twenty-two ODEs in the reduced order model is analyzed using the bifurcation analysis code BIFDD. In addition to the stability boundary in the design and operating parameter spaces, nature of bifurcation along the entire stability boundaries is also determined. Effects of various bifurcation parameters on the nature of bifurcation are analyzed. Results are presented for the effects of flux asymmetry on bifurcation characteristics as parameterized by the azimuthal mode feedback coefficient. To parameterize different flux shapes, an amplification factor F is introduced to vary the azimuthal mode feedback coefficient. In-phase oscillations result for smaller values of F ($F \sim 1$; azimuthally symmetric flux). Depending upon the values of other parameters, both sub- and supercritical bifurcations are predicted. However, as F is increased, leading to azimuthally asymmetric flux shapes, the real part of a second pair of complex conjugate eigenvalues increases, and this pair of eigenvalues approaches the imaginary axis. This pair, for large F and small values of N_{sub}, actually becomes the eigenvalue with the largest real part, leading to out-of-phase oscillations when the stability boundary is crossed. In this case, for parameter values studied so far, only supercritical bifurcations are predicted. The eigenvectors corresponding to the two pairs of complex conjugate eigenvalues suggest that one is responsible for in-phase oscillations, while the second is responsible for the out-of-phase oscillations. Results of numerical integrations confirm the findings of the semi-analytical bifurcation analyses.

1. INTRODUCTION

Boiling water reactors (BWRs) are known to experience large amplitude power and flow oscillations under specific operating conditions. Several instability incidents have been observed in operating BWRs [1-5]. Dynamics of BWRs have also been studied in controlled experiments in BWRs [6-8]. The interactions among thermal hydraulic features, such as vapor

generation rate, flow rate and pressure drop are sufficient to cause the so-called density wave oscillations (DWOs). The neutron kinetics, coupled with thermal-hydraulic features via void and fuel temperature feedback coefficients, introduces added complications to the dynamical behavior of BWRs.

Two different kinds of oscillations have been observed. The first one is called in-phase or core-wide oscillation. The power and flow in the entire reactor core in this case oscillate with almost the same frequency and phase. The second one is the out-of-phase or regional oscillation, where different parts of the core may oscillate out of phase, but the power and flow of the reactor as a whole will stay stationary or vary with much smaller amplitude.

In general, the instabilities in BWRs are studied using either large scale and highly detailed simulation codes or using reduced order models. Highly detailed simulation codes, such as RAMONA, RETRAN and RELAP, are used to simulate instability events observed in operating BWRs [1, 3-5]. Although such detailed analyses are helpful in understanding specific events, they are cumbersome and time-consuming, and of limited value in predicting parametric trends.

Reduced order models have the advantages that they can be analyzed in the time as well as frequency domain. Moreover, they can also be analyzed using bifurcation methods. Several reduced ordered models have been developed and studied. March-Leuba et al. [9] analyzed a very simple model in the frequency and time domain. This analysis was, later, extended to a two-channel model with fundamental as well as first azimuthal modes for neutronics analysis [10]. Karve et al. [11] and Karve [12] developed a BWR model, which consists of neutronics, fuel rod heat conduction and heated channel thermal hydraulics. Stability analyses and numerical simulations were carried out in different parameter spaces. Results of numerical integration were analyzed to deduce the nature of bifurcation. Another reduced order BWR model was developed by Munoz-Cobo et. al [13, 14] who used λ-mode, rather than ω-mode as used by Karve et al [12], for the neutronics part. Numerical simulations were performed and the out-of-phase oscillations were excited by increasing the azimuthal mode void feedback coefficient. Besides stability analyses and numerical simulations, bifurcation analyses were carried out by Tsuji [15] and Munoz-cobo [16]. Since these bifurcation studies were carried out using analytical asymptotic expansion methods, simple reduced order models of BWRs have been employed in these studies. Moreover, only a single parameter was varied as the bifurcation parameter, consequently limiting the scope of these analyses to a small region of the rather large parameter space. Rizwan-uddin [17] used the bifurcation analysis code BIFDD [18] to study the bifurcation characteristics of the simple BWR model proposed by March-Leuba et al [9], and explored the entire parameter space.

Some conclusions drawn from such studies are [4]: a) almost all the instability events occur in low flow/high power operating region of the reactor; b) radial and axial power shapes affect the stability and the resulting nature of oscillations.

With the aim of better understanding the instabilities in BWR, especially the out-of-phase oscillation phenomena, we have studied stability and bifurcation behavior of the much more detailed model developed by Karve et. al [11] using the bifurcation analysis code, BIFDD. We first determine the stability boundaries earlier obtained by Karve et al. [11, 12]. We determine the nature of bifurcation along the stability boundaries as well, and obtain these results in the entire parameter space. Role of the pairs of complex conjugate eigenvalues with largest and second largest real parts in determining the in-phase and out-of-phase oscillations is analyzed. Numerical simulations are carried out, which further confirm the results of stability and bifurcation analyses.

This paper is organized as follows. In section 2, the two-channel two-mode model developed by Karve et. al [11] is briefly reviewed. Poincare-Andronov-Hopf (PAH) bifurcation theory [19, 20] and the bifurcation analysis code BIFDD [18] are discussed in section 3. In section 4, results of the stability and bifurcation analyses are presented. Numerical simulation results, stability boundaries and nature of bifurcation are also discussed. Conclusions are drawn and the paper is summarized in the last section.

2. MODEL DESCRIPTION

The reduced order, two-channel BWR model, developed by Karve et. al [11], in which each channel represents one half of the reactor core, is comprised of three sub-models: neutronics, fuel rod heat conduction and heated channel thermal-hydraulics. A modal neutron kinetics model, with fundamental and first azimuthal modes, is employed. The governing neutron kinetics equations are coupled with those of heat conduction and heated channel thermal hydraulics via fuel rod temperature feedback coefficients and void feedback coefficients. Because detailed derivations of the sub-models are available in Refs. [11] and [12], only the neutronics part, which is most relevant to the results presented here, is discussed in detail. The other two parts are only briefly reviewed.

2.1 NEUTRONICS

The modal expansion method is used to develop the governing ordinary differential equations from the matrix form of the one-group diffusion and one-delayed neutron precursor equations. These are written as

$$\frac{d\bar{Y}}{dt} = \bar{\bar{M}}\,\bar{Y} \tag{1}$$

where $\bar{\bar{M}} = \begin{bmatrix} v\nabla\cdot D(\bar{r},t)\nabla - v\Sigma_a(\bar{r},t) + (1-\beta)v\nu\Sigma_f(\bar{r},t) & \lambda \\ v\beta\nu\Sigma_f & -\lambda \end{bmatrix}$, $\bar{Y}(\bar{r},t) = \left[N(\bar{r},t), C(\bar{r},t)\right]^T$, and $N(\bar{r},t)$ and $C(\bar{r},t)$ are neutron density and precursor concentration. The fundamental mode in the

cylindrical coordinate is

$$\psi_0 = J_0(2.4048r/R)Sin(\pi z/L), \tag{2}$$

which is positive-definite and independent of the azimuthal angle θ. The first azimuthal mode of $\overline{\overline{M}}$ is given by [10]

$$\psi_1 = J_1(3.1834r/R)Sin(\pi z/L)Sin(\theta) \tag{3}$$

Following ω-mode approach, the steady-sate eigenvalue w_{ik} and eigenfunction ϕ_{ik} of $\overline{\overline{M}}_0$ satisfy

$$\begin{aligned} &\overline{\overline{M}}_0\bar{\phi}_{ik} = w_{ik}\bar{\phi}_{ik} \\ &\bar{\phi}_{ik} = \begin{bmatrix} 1 \\ v\beta\upsilon\Sigma_f/(w_{ik}+\lambda) \end{bmatrix}\psi_k, \quad i = 0,1, \quad k = 0,1 \end{aligned} \tag{4}$$

The expansion of the time and space-dependent density vector

$$\bar{Y}(\bar{r},t) = u_{00}(t)\bar{\phi}_{00}(\bar{r}) + u_{01}(t)\bar{\phi}_{01}(\bar{r}) + u_{10}(t)\bar{\phi}_{10}(\bar{r}) + u_{11}(t)\bar{\phi}_{11}(\bar{r}) \tag{5}$$

is substituted into equation (1) and the inner-product of both sides is taken with the adjoint vector $\bar{\phi}_{ik}^{+}$. The final form of the modal kinetics equation based on the ω-modes are given by

$$\begin{aligned} &\frac{dn_k(t)}{dt} = \omega_{ik}n_k(t) + (\omega_{1k} - \omega_{0k})u_k(t) + \sum_{m=0}^{1}\frac{\rho_{km}}{\Lambda_k}n_m(t) \\ &\frac{du_k(t)}{dt} = \omega_{1k}u_k(t) + \sum_{m=0}^{1}\frac{\rho_{km}}{\Lambda_{1k}}n_m(t) \end{aligned} \qquad k = 0,1 \tag{6}$$

where $n_k(t) = u_{0k}(t) + u_{1k}(t)$, $u_k(t) = u_{1k}(t)$ and $\Lambda_{ik} = \dfrac{\left\langle \bar{\phi}_{ik}^{+}(\bar{r}), \bar{\phi}_{ik}(\bar{r}) \right\rangle_V}{\left\langle \psi_k(\bar{r}), v\upsilon\Sigma_f(\bar{r})\psi_k(\bar{r}) \right\rangle_V}$. Λ_{ik} here is the effective neutron generation time, where $\langle\ \rangle_V$ denotes the inner product over the volume of the core. The reactivity satisfies the non-linear equation

$$\rho_{km}(t) = \sum_{l=0}^{1}\rho_{ext,kml} - c_{\alpha,kml}(\alpha_l(t) - \alpha_{o,l}) - c_{D,kml}(T_{avg,l}(t) - T_{avg,o,l}) \tag{7}$$

where $\rho_{ext,kml}$ is the control-rod induced reactivity, $\alpha_l(t)$ and $T_{avg,l}(t)$ are void fraction and average fuel temperature, respectively. The form of the void and fuel temperature feedback coefficients are given by

$$c_{\alpha,kml} = c_{\alpha,l}\frac{\left\langle \psi_k(\bar{r}), v\nabla.\nabla\psi_m(\bar{r}) \right\rangle_{V_l}}{\left\langle \psi_k(\bar{r}), v\upsilon\Sigma_f(\bar{r})\psi_k(\bar{r}) \right\rangle_V} \tag{8}$$

$$c_{D,kml} = c_{D,l} \frac{\left\langle \psi_k(\bar{r}), v\psi_m(\bar{r}) \right\rangle_{V_l}}{\left\langle \psi_k(\bar{r}), v\upsilon\Sigma_f(\bar{r})\psi_k(\bar{r}) \right\rangle_V} \tag{9}$$

where $\langle\ \rangle_{V_l}$ is the inner product over the volume of the part of core represented by channel l; and $c_{\alpha,l}$ and $c_{D,l}$ are the typical values of void and fuel temperature feedback coefficients.

2.2 HEAT CONDUCTION AND CHANNEL THERMAL HYDRAULICS

In the fuel rod heat conduction part, the power density for each channel is given by

$$q_l''(t) = c_q (n_0(t) + \xi_l n_1(t)) \tag{10}$$

where c_q is a constant translating the dimensionless neutron density to power density. Volume factor $\xi_l = \langle 1, \psi_1(r) \rangle_{V_l} / \langle 1, \psi_0(r) \rangle_{V_l}$ denotes the contribution of channel l to the total power. Because the azimuthal mode $\psi_1(\bar{r})$ is of different sign for ($0 < \theta < \pi$) and ($\pi < \theta < 2\pi$) halves of the core, the sign of ξ_l is different for $l = 0, 1$. Thus, $\xi_l n_1(t)$ represents pure out-of-phase oscillation part in the power density.

Due to large temperature gradient in the fuel rod, a piecewise quadratic temperature distribution is assumed. Variational principle is used to derive the ODEs for the expansion parameters of the quadratic profile from the cylindrical heat conduction equations [12].

In the heated channel thermal hydraulics, similar to the fuel rod heat conduction, quadratic spatial variations are assumed for water enthalpy in the single-phase region, and for steam quality in the two-phase part. Homogeneous two-phase flow model is presently used to model the two-phase flow. Ordinary differential equations (ODEs) for the expansion coefficients of the quadratic spatial variation are derived by using the weighted-residual approach to the energy equations in the single phase and two-phase regions. The momentum equations are integrated over the whole flow channel to obtain the ODE for the inlet velocity.

The BWR model is comprised of 22 non-linear ODEs. The vector of dependent variables consists of [$a_{1,0}(t)$, $a_{2,0}(t)$, $s_{1,0}(t)$, $s_{2,0}(t)$, $v_{inlet,0}(t)$, $T_{11,0}(t)$, $T_{12,0}(t)$, $T_{21,0}(t)$, $T_{22,0}(t)$, $a_{1,1}(t)$, $a_{2,1}(t)$, $s_{1,1}(t)$, $s_{2,1}(t)$, $v_{inlet,1}(t)$, $T_{11,1}(t)$, $T_{12,1}(t)$, $T_{21,1}(t)$, $T_{22,1}(t)$, $n_0(t)$, $u_0(t)$, $n_1(t)$, $u_1(t)$]. Stability and bifurcation analysis of this model will be carried out in the section below.

3. POINCARE-ANDRONOV-HOPF BIFURCATION (PAH-B) ANALYSIS

2.1 PAH-B THEOREM

It is well known that the stability of an autonomous dynamical system is determined by the Jacobian of the governing ODEs. The fixed point of the system is stable only if real parts of all the eigenvalues of the Jacobian are negative. Otherwise, the fixed point is unstable. Although the stability analyses can determine when the fixed points of the system of ODEs lose their stability, linear analysis is not enough to determine if the periodic solutions that might be resulted will be stable or unstable. The PAH bifurcation theorem, on the other hand, can be used to explain the emergence of periodic solutions. (The term "bifurcation" is used to indicate "a qualitative change in the features of a system, such as the number and type of solutions" [20].) It states that a family of periodic solutions bifurcate from a fixed point as an operating parameter λ (called bifurcation parameter) is varied, and the following two conditions [19] are satisfied as λ approaches a critical value $\lambda_{critical}$:

a) a pair of pure imaginary eigenvalues ($\pm i\omega_0$) of the Jacobian of the system exist and the real parts of all the other eigenvalues are negative.
b) the real parts cross the imaginary axis with non-zero speed with respect to the bifurcation parameter λ, i.e. $\left.\frac{d(real\ part)}{d\lambda}\right|_{\lambda=\lambda_{critical}} \neq 0$.

The periodic solution, which is indexed by a constant ε, will exist in the vicinity of the critical bifurcation parameter $\lambda_{critical}$. Its form is given by

$$\overline{X}(t;T) = \overline{X}_{ss} + \varepsilon e^{\frac{2\pi i}{T}t}\overline{P} + O(\varepsilon^2) \tag{11}$$

where $\overline{X}_{ss}$ is the fixed point of the system, $\overline{P}$ is the eigenvector corresponding to the pure imaginary eigenvalue $i\omega_0$, and $\overline{P}$ is normalized such that its first non-zero element is equal to one. The period *T*, and the relationship between the value of λ corresponding to this periodic solution, $\lambda_{critical}$, and oscillation amplitude ε are given by

$$T = \frac{2\pi}{\omega_0}\left(1 + \tau_2\varepsilon^2 + O(\varepsilon^4)\right) \tag{12}$$

$$\lambda = \lambda_{critical} + \mu_2\varepsilon^2 + O(\varepsilon^4) \tag{13}$$

2.2 FLOQUET THEORY

The stability of the periodic solutions, whose existence is guaranteed by the PAH bifurcation theorem, is determined by the Floquet theory [20], in the same way as that of fixed points, i.e. by introducing a perturbation to the periodic solution, and then analyzing whether the perturbation grows or decays. The mathematics finally leads to the evaluation of Floquet exponents. The perturbations decay if all the Floquet exponents have negative real parts. Otherwise they grow in magnitude. Moreover, it has been shown that one of the Floquet exponent is exactly zero, and a second one is given by [19]

$$\beta = \beta_2\varepsilon^2 + O(\varepsilon^4) \tag{14}$$

as λ approaches $\lambda_{critical}$. If $\beta_2 > 0$, the periodic solution is unstable leading to what is usually called subcritical PAH bifurcation. Otherwise, if $\beta_2 < 0$, the periodic solution is stable and the corresponding bifurcation is called supercritical PAH bifurcation. The bifurcation, at the critical value of the bifurcation parameter, is either supercritical or subcritical but not both.

2.3 BIFDD

To determine the nature of bifurcation along the stability boundaries, the values of μ_2, τ_2 and β_2 must be evaluated. Center manifold theorem [19], which can be used to project the local characteristics of a set of *n* nonlinear ODEs onto a two dimensional manifold, and asymptotic expansion methods are used to evaluate these parameters. This is a formidable task for the set of ODEs that model the BWRs. To simplify the task of mathematical manipulations, a code called BIFDD has been developed by Hassard et. al [18]. The code is based on numerical evaluation of the functions (right hand side of the set of ODEs), the Jacobian and higher order derivatives. A user defined subroutine, which provides the analytical form of the set of nonlinear ODEs and its Jacobian is required, and an operating parameter needs to be chosen as the bifurcation parameter. The code then determines the critical value of the bifurcation parameter, $\lambda_{critical}$, and the values of ω_0, μ_2, τ_2 and β_2.

Because BIFDD can determine only one point on the stability boundary and its associated nature of PAH bifurcation, to find the stability boundaries in, say, a two-dimensional parameter

space, an additional loop is added, in which a second parameter can be incremented. In the inner loop, all the operating parameters except the bifurcation parameter are fixed and BIFDD is called to evaluate the critical value of the bifurcation parameter and its associated ω_0, μ_2, τ_2 and β_2. The second parameter is then incremented in the outer loop and the same process is repeated. Thus, an entire stability boundary (SB) in two-dimensional parameter space and the nature of bifurcation along the SB is determined.

Results of stability and bifurcation analyses as well as numerical simulations are presented in the next section.

4. RESULTS AND DISCUSSIONS

It is clear from equations (8) and (9) that the feedback coefficients depend upon the inner products of the fundamental and azimuthal modes. In the model developed by Karve et al. [12], the values of feedback coefficients are calculated using the shapes of modes given by equations (2) and (3). These modes are the result of a homogenized core. However, inhomogeneities in neutron cross-section and/or asymmetric control rod insertion in the core may change the shapes of the modes, and therefore may change the feedback coefficients. Such changes have been observed in simulations of some instability events using large system codes [4-5]. Miro et al. [4] indicated that the fundamental mode power distributions tend to generate in-phase oscillations; while the bowl-shaped power distributions with a local minimum at the core center tend to produce out-of-phase or regional oscillations. To address the effect of different shapes of modes, parametric approach used by Munoz-Cobo et al. [14], has been adopted. Thus the azimuthal mode feedback coefficients are multiplied by an amplification factor *F*, that is,

$$c_{\alpha,kml} = F \cdot c_{\alpha,l} \frac{\left\langle \psi_k(\bar{r}), v\nabla.\nabla\psi_m(\bar{r}) \right\rangle_{V_l}}{\left\langle \psi_k(\bar{r}), v\upsilon\Sigma_f(\bar{r})\psi_k(\bar{r}) \right\rangle_V} \tag{15}$$

$$c_{D,kml} = F \cdot c_{D,l} \frac{\left\langle \psi_k(\bar{r}), v\psi_m(\bar{r}) \right\rangle_{V_l}}{\left\langle \psi_k(\bar{r}), v\upsilon\Sigma_f(\bar{r})\psi_k(\bar{r}) \right\rangle_V} \tag{16}$$

and the effects of modal reactivity interactions are studied parametrically. Intuitively, if *F* is small, the feedback coefficients of the azimuthal mode are small, and BWR will tend to develop in-phase or global oscillations. However, if *F* is large, the feedback coefficients of the azimuthal mode are also large, and BWR will more likely experience out-of-phase or regional oscillations. Results for stability and bifurcation analyses and numerical simulations for *F*=1 case are presented in section 4.1. Effect of *F* on the stability characteristics and dynamics of BWRs are presented in section 4.2. All parameter values not explicitly specified are from Appendix H of Ref. [12].

4.1 RESULTS: $F = 1$ CASE

We first determine the SB in the N_{sub} — ΔP_{ext} parameter space for $\rho_{ext} = 0$, where, N_{sub} is the non-dimensional subcooling number, ΔP_{ext} is the non-dimensional pressure drop over the flow channel, and ρ_{ext} is the control rod induced fundamental mode reactivity. The SB separates a stable region from an unstable one. In the stable region, all the eigenvalues of the Jacobian matrix have negative real parts and the fixed point is stable. In the unstable region, however, at least one eigenvalue of the Jacobian matrix has positive real part and the fixed point is unstable. The SBs we obtain are identical to those obtained earlier by Karve et al. [12], and a typical SB is shown in Figure 1 (a). Next, the results of the bifurcation analysis are presented in the form of constant amplitude oscillation curve in the N_{sub} — $(\Delta P_{ext} - \Delta P_{ext,critical})$ parameter space. The curve plotted in Figure 1 (b) corresponds to the points in the parameter space whose index constant of the periodic solution is $\varepsilon = 0.15$, that is, the amplitudes of the periodic solutions on this curve, given by the magnitude of $\varepsilon\overline{P}$, are 15% of the magnitude of the eigenvector. For this reason, this curve is also called the *15% oscillation curve*. The PAH bifurcation (PAH-B) theorem states that the bifurcation is *supercritical* when this curve is in the unstable region, and *subcritical* when it is in the stable region. Hence, in the upper part of the stability boundary for $N_{sub} > 1.85$, where the oscillation curve is in the stable region, the bifurcation is subcritical. Thus, the small amplitude perturbations will decay, but "large" amplitude perturbations may grow. For $0.5 < N_{sub} < 1.85$, the oscillation curve is in the unstable region and the bifurcation is thus supercritical. That means the periodic solution is stable, and the perturbation will evolve to this stable periodic solution. For even lower values of N_{sub} (< 0.5), the 15 % oscillations curve goes back to the stable region, and the bifurcation is hence subcritical. The back and forth transition between supercritical and subcritical PAH-B in the low N_{sub} region might explain the reason behind stable amplitude oscillation in some BWR instability cases, and the growing amplitude oscillation (until scram) for others.

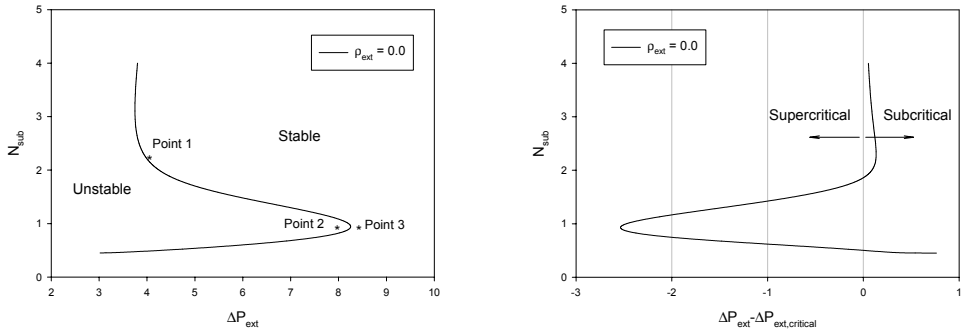

(a) (b)

Figure 1. Stability and bifurcation analyses for $F = 1$, (a) SB; (b) 15% oscillation curve

To investigate the time evolution, and validate the results of BIFDD, three points are selected in the parameter space for the numerical simulations. Figures 2, 3, and 4 show the results of the numerical simulations for these points. Point 1 is in the subcritical bifurcation region on the stable side of the SB. According to PAH-bifurcation theorem, large perturbations, when operating at point 1 in the parameter space, may lead to increasing amplitude oscillations. Point 2, however, is in the supercritical bifurcation region on the unstable side of the SB. Hence perturbations are expected to evolve to stable amplitude oscillations. Point 3 is in the supercritical bifurcation region but on the stable side of the SB. Hence, perturbations are expected to decay. Time evolution plots of n_0, n_1 and $v_{inlet,0}$ shown in Figures 2, 3, and 4 confirm these predictions. Numerical simulations also show that the oscillations plotted in Figures 2, 3, and 4 are almost pure in-phase oscillations, where amplitude of n_1 is much smaller than that of n_0 and $v_{inlet,0}$ and $v_{inlet,1}$ (non-dimensional inlet velocities), and both channels oscillate with the same phase and amplitude. In this case, the behavior of the two-channel two-mode model is similar to a one-channel point-reactor one.

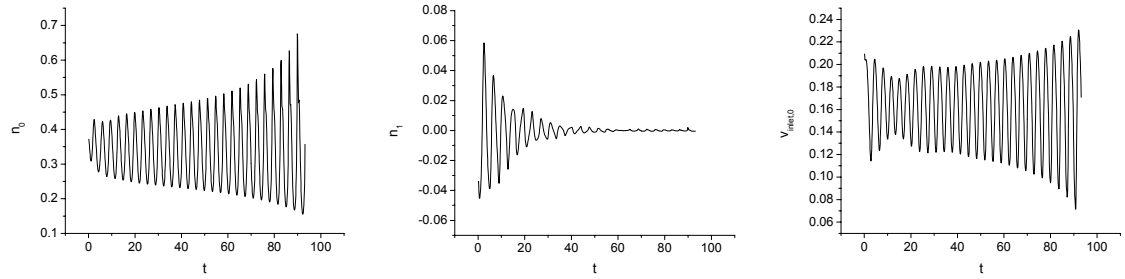

(a) (b) (c)

Figure 2. Time evolution of n_0, n_1 and v_{inlet} at point 1 ($N_{sub} = 2.2303$, $\Delta P_{ext} = 3.9840$)

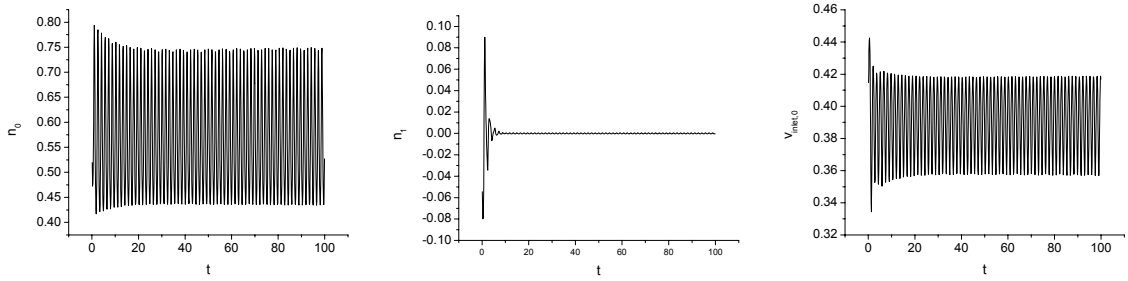

(a) (b) (c)

Figure 3. Time evolution of n_0, n_1 and v_{inlet} at point 2 ($N_{sub} = 1.0000$, $\Delta P_{ext} = 8.1000$)

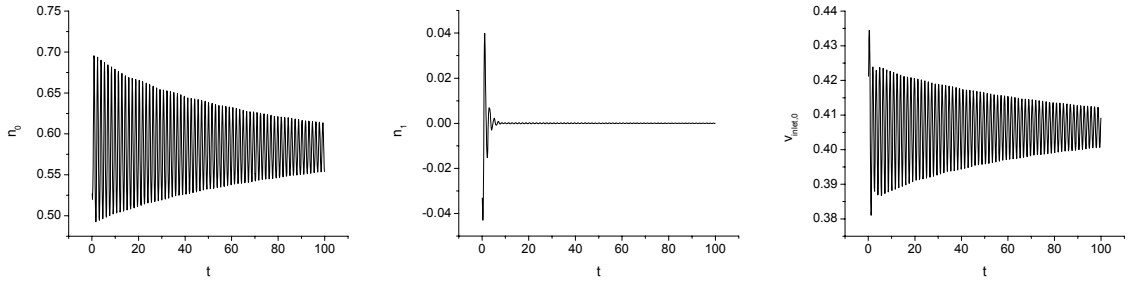

(a) (b) (c)

Figure 4. Time evolution of n_0, n_1 and v_{inlet} at point 3 ($N_{sub} = 1.0000$, $\Delta P_{ext} = 8.5000$)

4.2 RESULTS: CASES $F > 1$

The results of the parametric analysis of different power distributions, as represented by the values of the amplification factor *F*, are presented in this section. Figure 5 shows SB and $\varepsilon =$ 0.15 curves for *F = 2.0, 3.5* and *4.6*. The SBs are so close that they can not be distinguished from each other. Also, the constant amplitude oscillation curves shown in Figure 5 (b) are very

close. However, the results of numerical simulations for parameter values corresponding to point 3 in Figure 5 (a) for F = 2.0, 3.5 and 4.6, shown in Figures 6, 7 and 8 suggest that the system is becoming increasingly less stable as F is increased. Specifically, the amplitude of n_1 does not decay as fast for large values of F as it does for smaller values of F. Slight beating of $v_{inlet,0}$ is also observed in Figure 8 (c). Results of the numerical simulations shown in Figures 6-8 can not be explained by the pair of conjugate complex eigenvalues with the largest real part (which are considered in the PAH-B theorem), and clearly indicates that, as F is increased, a second pair of eigenvalues is approaching the imaginary axis.

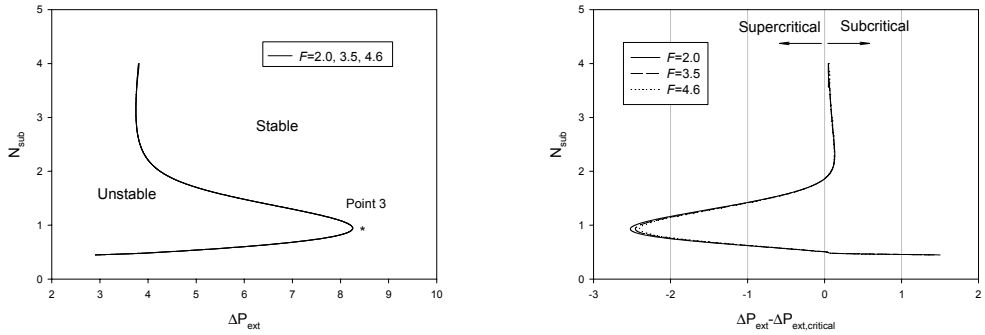

(a) (b)

Figure 5. SBs and ε = 0.15 curves for F = 2.0, 3.5, and 4.6

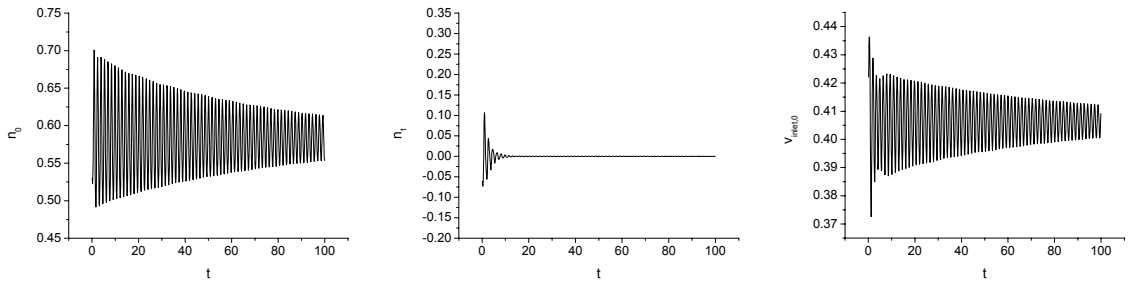

(a) (b) (c)

Figure 6. Time evolution of n_0, n_1 and v_{inlet} for parameter values corresponding to point 3 (N_{sub} = 1.0000, ΔP_{ext} = 8.5000), when F = 2.0

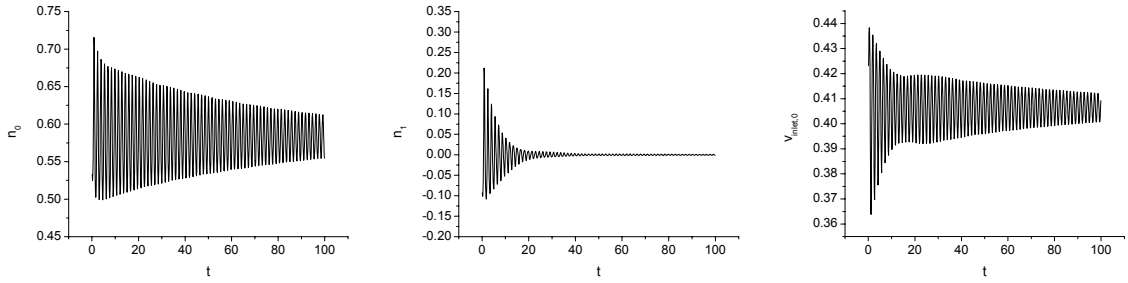

(a) (b) (c)

Figure 7. Time evolution of n_0, n_1 and v_{inlet} for parameter values corresponding to point 3 (N_{sub} = 1.0000, ΔP_{ext} = 8.5000), when F = 3.5

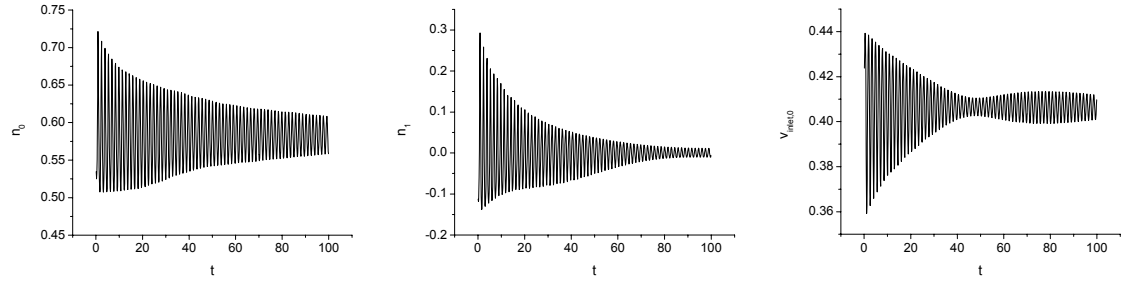

(a) (b) (c)

Figure 8. Time evolution of n_0, n_1 and v_{inlet} for parameter values corresponding to point 3 (N_{sub} = 1.0000, ΔP_{ext} = 8.5000), when F = 4.6

To study this secondary frequency and identify its relationship with the amplitude of n_1 and the out-of-phase oscillations, the bifurcation code BIFDD was modified to evaluate all eigenvalues of the Jacobian matrix. Table 1 lists the pair of complex conjugate eigenvalues e_1 and e_2 with the largest and the second largest real parts, respectively. Since there are real eigenvalues between the two complex conjugate pairs, the order of the eigenvalues sorted by their real parts is also indicated. Hence, for F = 1 there are six real eigenvalues with magnitude a, $-0.7324<a<0.0000$. These eigenvalues correspond to a point on the SB in Figure 5 with N_{sub} = 1.0000 and ΔP_{ext} = 8.2085, which is on the SB on a horizontal line that pass through point 3.

Table 1 Eigenvalues e_1 and e_2

	Eigenvalue e_1			Eigenvalue e_2		
F	Real part	Imag. part	Order	Real part	Imag. part	Order
1.0	0.0000	±4.1560	1	-0.7324	±3.1892	8
2.0	0.0000	±4.1560	1	-0.3678	±3.5476	6
3.5	0.0000	±4.1563	1	-0.1114	±3.9754	2
4.6	0.0000	±4.1537	1	-0.01232	±4.2220	2

Table 1 shows that the real part of e_2 becomes increasingly larger as the amplification factor F is increased. Six real eigenvalues between e_1 and e_2 for the $F = 1$ case are crossed, and for $F = 3.5$, e_2 becomes the eigenvalue with the second largest real part. The value of the second largest real part for $F = 4.6$ is so close to zero that it is expected to interact with the fundamental frequency. The two frequencies (4.1537 and 4.2220) are slightly different, hence explaining the *beating* phenomena observed in the numerical simulations of $v_{inlet,0}$ in Figure 8 (c). The ratio of the two frequencies correctly predicts the period of the *beat*.

To study the characteristics of the oscillations produced by the two pairs of complex conjugate eigenvalues, the elements corresponding to n_0 and n_1 in the eigenvectors corresponding to e_1 and e_2 were calculated. They are shown in Tables 2 and 3.

Table 2 Elements corresponding to n_0 and n_1 in the eigenvector corresponding to e_1

	n_0			n_1			$\lvert n_0\rvert/\lvert n_1\rvert$
F	Real	Imaginary	Magnitude	Real	Imaginary	Magnitude	
1.0	1.3656	4.8667	5.0546	0.004590	0.01369	0.01444	350.04
2.0	1.3615	4.8533	5.0407	0.01231	0.03922	0.04111	122.61
3.5	1.3482	4.7732	4.9600	0.03740	0.1920	0.1956	25.36
4.6	1.6890	5.1131	5.3848	-0.6087	-0.4666	0.7670	7.02

Table 3 Elements corresponding to n_0 and n_1 in the eigenvector corresponding to e_2

	n_0			n_1			$\lvert n_1\rvert/\lvert n_0\rvert$
F	Real	Imaginary	Magnitude	Real	Imaginary	Magnitude	
1.0	-0.009630	-0.01334	0.01645	2.7592	3.9449	4.8140	292.64
2.0	-0.01475	-0.03072	0.03407	2.8850	6.3208	6.9481	203.94
3.5	-0.02896	-0.1192	0.1227	2.6818	8.5689	8.9788	73.18
4.6	0.2584	0.2299	0.3459	1.8988	8.9610	9.1600	26.48

In eigenvector corresponding to e_1, the magnitudes of the elements of n_0, shown in Table 2, are

much larger than those of elements of n_1. However, the trend is reversed (in Table 3) for eigenvalue e_2. As the value of F is increased, the difference of magnitudes between the two elements, in both tables, is decreasing. However, the ratio of the magnitude of element of n_0 to n_1 for eigenvalue e_1, and the ratio of magnitude of element of n_1 to n_0 for eigenvalue e_2 are still large. Because the magnitudes of the elements of the eigenvector determine the amplitudes of oscillations of different variables (equation (11)), this result suggests that in the oscillation produced by the eigenvalue e_1, the amplitude of oscillation of n_0 is much larger than that of n_1, and hence the oscillations are dominated by the in-phase component. Also, the amplitude of oscillation of n_1 will be much larger than that of n_0 in oscillations produced by the eigenvalue e_2, and hence the oscillations will be mainly out-of-phase. In order to avoid confusion, the pair of eigenvalues for which magnitudes of element of n_0 in the corresponding eigenvector is much larger than that of element of n_1, will be called the fundamental mode eigenvalues ($a_f + i\, w_f$), and the other pair will be called the first azimuthal mode eigenvalues ($a_a + i\, w_a$).

It is clear that the two pairs of complex conjugate eigenvalues — with the largest and second largest real part — are responsible for the fundamental and the first azimuthal mode (in-phase and out-of-phase) oscillations, respectively. It is also quite clear that as F is further increased beyond 4.6, the pair of complex conjugate eigenvalues with the second largest real part (the azimuthal mode eigenvalue) will cross the fundamental mode eigenvalue. Figure 9 (a) shows the SB for F = 5.0. The SB (solid line) in Fig 9 (a), on which the real part of the rightmost eigenvalues is zero, is comprised of two curves that meet at the point T (N_{sub} = 1.177, ΔP_{ext} = 7.618). Above this point, the eigenvalues with the largest real part along the SB are the fundamental mode eigenvalues, that is, a_f = 0 and a_a < 0. However, for N_{sub} < 1.177 (below the point T), the eigenvalues with the largest real parts along the SB are the azimuthal mode eigenvalues (a_a = 0 and a_f < 0). The dotted line in Figure 9 (a) denotes the boundary along which the real part of the second rightmost pair of complex conjugate eigenvalue is zero. (This means that the rightmost pair of complex conjugate eigenvalue has positive real part). The dotted curve is also comprised of two branches. Along the branch above the point T, the real parts of the azimuthal mode eigenvalues are zero (a_a = 0 and a_f > 0). However, along the

lower branch, the real parts of fundamental mode eigenvalues are zero (a_f = 0 and a_a > 0). Hence, the parameter space is divided into four parts, denoted by letter A, B, C and D [10]. Region C and A are respectively stable and unstable (for both in-phase and out-of-phase mode oscillation). In region B, the fundamental mode (in-phase) is unstable while the first azimuthal mode (out-of-phase) is stable. While in region D, the first azimuthal mode (out-of-phase) is unstable, but the fundamental mode (in-phase) is stable. These results are similar to those obtained using a simple model by March-Leuba et al. [10]. Another point of concern (at such large values of *F*; not for smaller values of *F*) is the fact that the two pairs of eigenvalues are very close to each other along the whole SB.

The effect of *F* = 5 on the bifurcation characteristic was also studied. Results of the bifurcation analyses are presented in Figure 9 (b) in the form of 5% oscillation amplitude curve in N_{sub} — $(\Delta P_{ext} - \Delta P_{ext,critical})$ space. The solid line corresponds to the SB (solid line) in Figure 9 (a), while the dotted curve corresponds to the dotted curve in Figure 9 (a) (i.e., to the second rightmost eigenvalue crossing the imaginary axis). In Figure 9 (b), a jump in the 5% oscillation curve (solid line) is at the point T, because of the fact that at this value of N_{sub}, both the fundamental and first azimuthal mode eigenvalues have zero real parts. The 5% oscillation curve for N_{sub} > 1.177 is determined using the fundamental mode eigenvalues, while for N_{sub} < 1.177 they must be determined using the first azimuthal mode eigenvalues. Note that the 5% oscillation curve for each pair of eigenvalue is smooth over the entire range of N_{sub}. However, only a segment (the solid part) of each is relevant. (Condition (a) of PAH-B theorem is violated along the dotted line.) Though the PAH-B theorem is strictly applicable only along the solid lines in Figure 9, results of the numerical simulations show that the conclusions regarding the stable and unstable periodic solutions may be applicable even to the second pair of complex conjugate eigenvalues that cross the imaginary axis *right behind* the first pair.

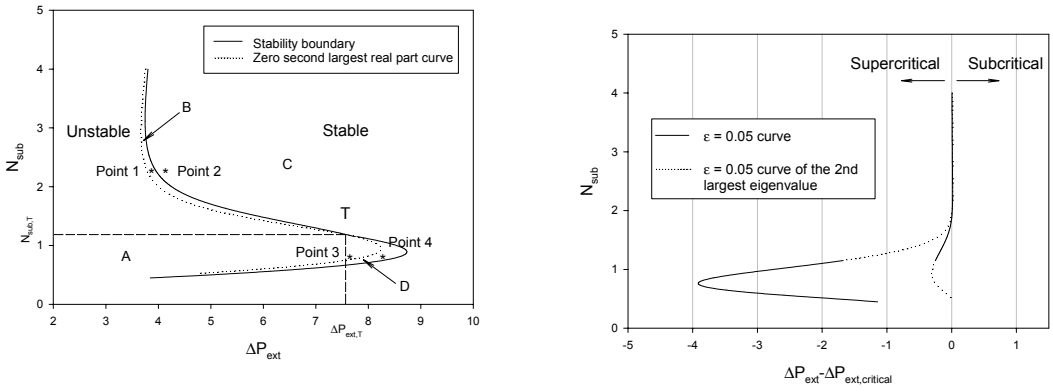

(a) (b)

Figure 9. The SB (a) and 5% oscillation amplitude curves (b) of the eigenvalues with the largest and second largest real parts (F = 5.0)

Results of the numerical simulation for parameter value at point 1 (N_{sub} = 2.2303, ΔP_{ext} = 3.9000), 2 (N_{sub} = 2.2303, ΔP_{ext} = 3.9834), 3 (N_{sub} = 0.8000, ΔP_{ext} = 7.6000), and 4 (N_{sub} = 0.8, ΔP_{ext} = 8.2000) are shown in Figure 10-13. Points 1-4 are shown in Figure 9 (a). It is clear that the dominant oscillations in the high and low N_{sub} regions are different. In the high N_{sub} region, the in-phase oscillations are dominant because the critical eigenvalues on the SB are the fundamental mode ones. In the low N_{sub} region, however, the out-of-phase oscillations are dominant because the critical eigenvalues are azimuthal mode ones. In the region around the intersection point, both the effect of the fundamental and azimuthal mode eigenvalues are evident. The oscillations in this region are combinations of both in-phase and out-phase in different strength.

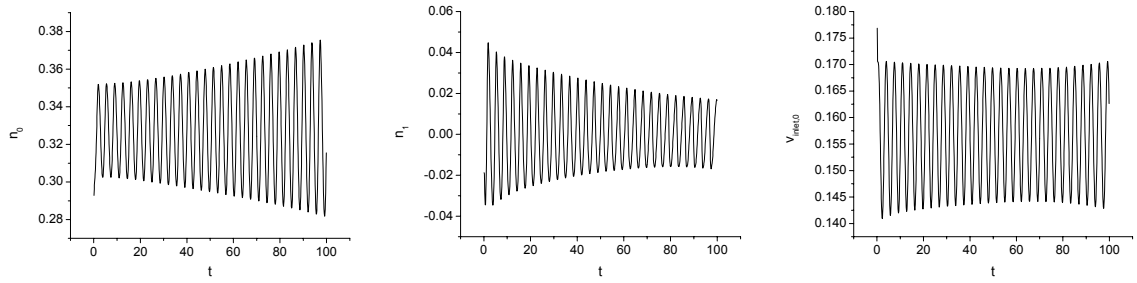

(a) (b) (c)

Figure 10. Time evolution of n_0, n_1 and v_{inlet} for parameter values corresponding to point 1

($N_{sub} = 2.2303,\ \Delta P_{ext} = 3.9000,\ F = 5.0$)

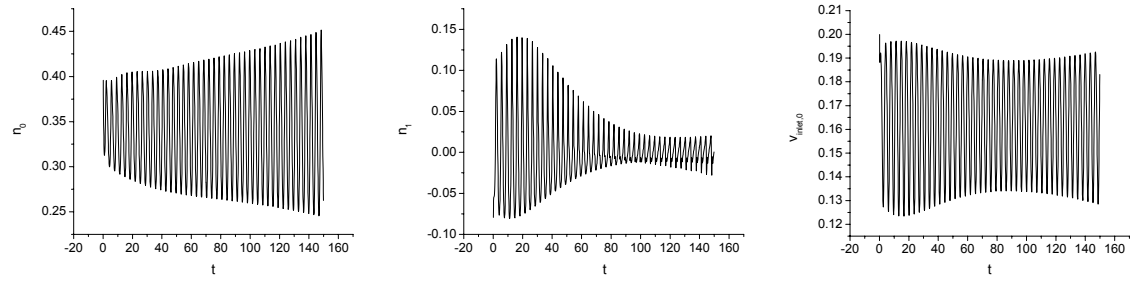

(a) (b) (c)

Figure 11. Time evolution of n_0, n_1 and v_{inlet} for parameter values corresponding to point 2

($N_{sub} = 2.2303,\ \Delta P_{ext} = 3.9840,\ F = 5.0$)

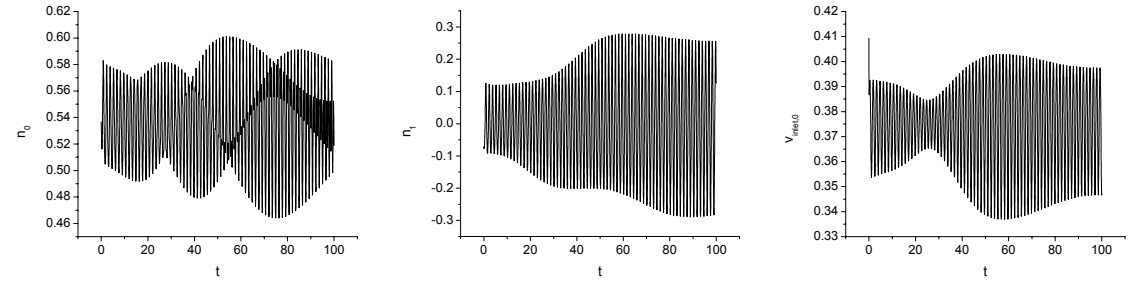

(a) (b) (c)

Figure 12. Time evolution of n_0, n_1 and v_{inlet} for parameter values corresponding to point 3

($N_{sub} = 0.8000,\ \Delta P_{ext} = 7.6000,\ F = 5.0$)

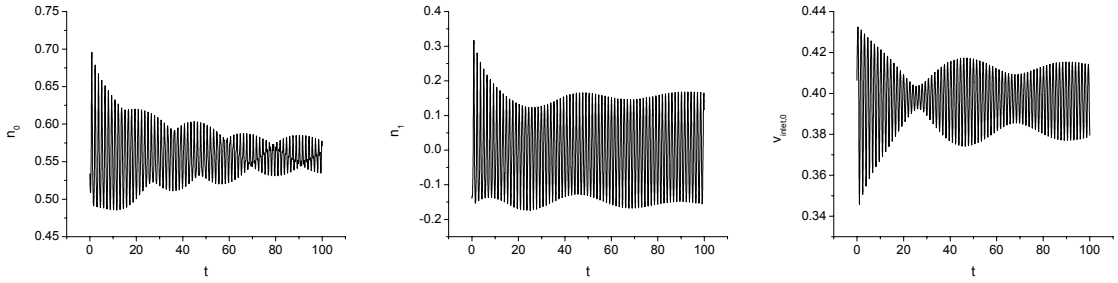

(a) (b) (c)

Figure 13. Time evolution of n_0, n_1 and v_{inlet} for parameter values corresponding to point 4

($N_{sub} = 0.8000$, $\Delta P_{ext} = 8.2000$, $F = 5.0$)

SUMMARY

Stability and bifurcation analyses of a two-channel, BWR model were carried out. The model includes fuel rod heat conduction, and single- and two-phase flow thermal hydraulics. Fundamental and first azimuthal modes are used to represent the neutron and delayed precursor concentrations. The BWR as a dynamical system is represented by twenty-two nonlinear, coupled ODEs. The stability boundary and the nature of PAH-B along this SB are computed by the bifurcation code BIFDD. Numerical integrations are also carried out.

For parameter values that correspond to azimuthally symmetric flux shapes, both sub- and supercritical bifurcations are found in regions of parameter space analyzed. It is found that bifurcation can switch from sub- to super- and back to subcritical over a narrow range of a single operating parameter (such as inlet subcooling). In the azimuthally symmetric flux shape case, only in-phase oscillations are found.

To capture the effects of different flux shapes and asymmetry in flux, the azimuthal mode feedback coefficients is multiplied by an amplification factor F. As the amplification factor F is increased, real part of a second pair of complex conjugate eigenvalues increases and approaches the imaginary axis. Magnitude of the corresponding eigenvectors suggests that this second pair of complex conjugate eigenvalues is responsible for the out-of-phase oscillations. As F is increased ($F = 2.0$, 3.5 and 4.6), numerical simulations show evidence of out-of-phase oscillations. Though still stable (decaying oscillations) the out-of-phase oscillations are increasingly slow in decaying as F is increased. Indeed the eigenvectors of the two pairs of complex conjugate eigenvalues show different types of oscillations. The oscillations produced by the pair of complex conjugate eigenvalues with the largest real part (for these relatively smaller values of F) are mainly in-phase, and those produced by the complex conjugate eigenvalues with the second largest real part are mostly out-of-phase.

Finally, as the parameter F is increased to about 5, for some values of inlet subcooling the pair of complex conjugate pair of eigenvalues associated with the out-of-phase oscillations reaches the imaginary axis (as the imposed pressure drop is increased) even before the eigenvalues associated with the fundamental mode oscillations. The nature of bifurcation in this case, for other rangers of parameter values studied, is predominantly supercritical. Numerical integrations confirm the results of the stability and bifurcation analyses.

The single unified model analyzed here clearly shows that it is capable of predicting in-phase and out-of-phase oscillations, as well as stable amplitude and growing amplitude oscillations. Thus, various type of instabilities and oscillations observed in operating reactors or those observed under controlled conditions have been successfully modeled.

ACKNOWLEGEMENTS

This work was supported in part by a grant from U.S. DOE under grant number DE-FG07-00ID13923.

REFERENCES

1. F. Araya, K. Yoshida, M. Hirano, Y. Yabushita, "Analysis of a neutron flux oscillation event at LaSalle-2", *Nucl. Tech.*, **Vol. 93**, pp. 82-91(1991)
2. E.HIRUO, "WNP-2 Down after power oscillation that saw level swing about 24%", *Neucleonics Week*, pp.2-3 (Aug. 20, 1992).
3. Y. M. Farawila, D.W. Pruitt, P.E. Smith, "Analysis of the Laguna Verdu instability event", *ANS proc., 1996 National Heat Transfer Conf.*, Houston, Texas, Aug. 3-6 (1996), HTC-Vol. 9, pp. 198-202 (1996)
4. R. Miro, D. Ginestar, D. Hannig, G. Verdu, "On the regional oscillation phenomena in BWR's", *Progress in Nuclear Eneregy*, **Vol. 36**, No. 2, pp. 189-229 (2000)
5. G. Th. Analytis, D. Hennig, J.K.-H. Karlsson, "The physical mechanism of core-wide and local instabilities at the Forsmark-1 BWR", Nuclear Engineering and Design, Vol. 205, pp. 91-105 (2001)
6. E. Gialdi, S. Grifoni, C. Parmeggiani, C. Tricoli, "Core stability in operating BWR: operational experience", *Progress in Nuclear Energy*, **Vol. 15**, pp. 447-459 (1985)
7. B.G. Bergdahl, F. Reisch, R. Oguma, J. Lorenzen, F. Akerhielm, "BWR stability investigation at Forsmark 1", *Ann. Nucl. Energy*, **Vol .16**, No. 10, pp. 509-520 (1989)
8. T.H.J.J. Van Der Hagen, A.J.C. Stekelenburg, D.D.B. Van Bragt, "Reactor experiments on type-I and type-II BWR stability", *Nuclear Engineering and design*, **Vol. 200**, pp. 177-185 (2000)
9. J. March-Leuba, D.G. Cacuci, R.B. Perez, "Nonlinear dynamics and stability of boiling water reactors: part I-qualitative analysis", *Nucl. Sci. Eng.*, **Vol. 93**, pp. 11-123 (1986).
10. J. March-Leuba, E.D. Blakeman, "A mechanism for out-of-phase power instabilities in boiling water reators", *Nucl. Sci. Eng.*, **Vol. 107**, pp. 173-179 (1991).

11. A.A. Karve, Rizwan-uddin, J.J. Dorning, “Out of phase power oscillations in boiling water reactors”, *Proc. Of the Joint Int. Conf. On Mathematical Methods and Super-computing*, Saratoga Springs, NY, Oct. 5-9, 1997, Vol.2, pp. 1633-1647 (1997)
12. A.A. Karve, “Nuclear-coupled thermal-hydraulic stability analysis of boiling water reactors”, Ph.D. Dissertation, Virginia University (1999).
13. J.L. Munoz-Cobo, R.B. Perez, D. Ginestar, A. Escriva, G. Verdu, “Non linear analysis of out of phase oscillations in boiling water reactors”, *Ann. Nucl. Energy*, **Vol. 23**, No.16, pp, 1301-1335 (1996)
14. J.L. Munoz-Cobo, O. Rosello, R. Miro, A. Escriva, D. Ginestar, G. Verdu, “Coupling of density wave oscillations in parallel channels with high order modal kinetics: application to BWR out of phase oscillations”, *Ann. Nucl. Energy*, **Vol. 17**, pp. 1345-1371 (2000)
15. M. Tsuji, K. Nishio, M. Narita, “Stability analysis of BWRs using bifurcation theroy”, *J. Nucl. Sci. Tech.*, Vol**. 30**, pp.1107-1119, (1993)
16. J.L. Munoz-Cobo, G. Verdu, “Application of Hopf bifurcation theory and variational methods to the study of limit cycles in boiling water reactors”, *Ann. Nucl. Energy*, **Vol. 18, No. 5**, pp. 269 (1991).
17. Rizwan-uddin, “Sub- and supercritical bifurcation and turning points in a simple BWR model”, *Proc. PHYSOR-2000 ANS int. Top. Meeting on Adv. In Reactor Phys. And Math.* Pittsburgh, May 7-11 (2000).
18. B.D. Hassard, “A code for bifurcation analysis of autonomous delay-differential systems”, *Proc. Oscillation, Bifurcation and Chaos, Canadian Mathematical Society*, pp. 447-463 (1987)
19. B.D. Hassard, N.D. Kazarinoff, Y.H. Wan, *Theory and applications of Hopf bifurcation*, Cambridge University Press, New York (1981).
20. A.H. Nayfeh, B. Balachandran, *Applied nonlinear dynamics*, John Wiley & Sons, Inc., New York (1995).